IJFANS INTERNATIONAL JOURNAL OF FOOD AND NUTRITIONAL SCIENCES

ISSN PRINT 2319 1775 Online 2320 7876

 Volume 11, Sp.Iss 6 , 2022

The Influence of Slip Effects on the Flow of MHD Cu-Al2O3 Hybrid Nanofluid Over a Moving Plate

M. Radha Madhavi[1], M. Veeranjaneyulu[2], N. Srimannarayana[1]

[1]*Department of Engineering Mathematics, College of Engineering, Koneru Lakshmaiah Education Foundation (KLEF), Vaddeswaram, Green fields, Guntur, Andhra Pradesh, India -522302*

[2]*Department of physics, Sir CRR College of Engineering, Eluru, Andhra Pradesh, India*

Corresponding author : mrmadhavi5@gmail.com

DOI : 10.48047/IJFANS/11/S6/028

Abstract. The focus of this study revolves around the dynamics of MHD hybrid nanofluid flow and heat transfer on a contracting plate embedded in porous media, accounting for Darcy slip and thermal radiation effects. The investigation employs a blend of copper (Cu) and aluminum oxide (Al_2 O_3) nanoparticles suspended in water (H_2O) as the fundamental working fluid. By employing mathematical transformations, the complex partial differential equations are transformed into a set of ordinary differential equations (ODEs). These ODEs are subsequently solved numerically using the function-bvp4c within the MATLAB software tool, exploring multiple scenarios across various key parameters. This analysis carries significant importance as it sheds light on the thermal behaviour of the Cu- Al_2 O_3/ H_2O nanofluid mixture under the influence of crucial physical parameters with magnetic field M, heat generation parameter β, velocity slip parameter A, thermal radiation parameter R, thermal slip parameter B, porosity parameter P, and suction parameter S. The research outcomes are both contemporary and pioneering, offering a wealth of practical applications within modern industries.

Keywords: Nanoparticles,magnetic field,porous media,thermal radiation effects

1. Introduction

Enhancing heat transfer applications for substantial energy and cost reductions is a pivotal goal within various industries. In today's rapidly evolving landscape of science and technology, industries prioritize high performance, precision, and extended product lifetimes. Consequently, numerous researchers are keenly interested in investigating heat and mass transfer techniques. Some of these investigators have turned their attention to nanofluids as alternatives to conventional fluids to enhance thermal properties. Recent advancements have revealed the potential of hybrid nanofluids, which involve the combination of two distinct nanoparticles in a base fluid. This emerging class of hybrid nanofluids has garnered significant attention among international researchers due to its wide-ranging applications in fields such as medicine, transportation, microelectronics, naval engineering, defines, and more.

Hybrid nanofluids have gained extensive attention in both experimental and numerical research due to their remarkable thermal and energy-related properties. These nanofluids are composed of hybrid nanoparticles, which are derived from a combination of different nanoparticle types, including metal oxides like hematite, magnetite, alumina, copper oxide, carbon materials like carbon nanotubes, graphite, and multi-walled carbon nanotubes, as well as metals such as silver, copper, or metal carbides. Suresh et al. [1,2] conducted a

ISSN PRINT 2319 1775 Online 2320 7876
 Volume 11, Sp.Iss 6 , 2022

comprehensive examination of the advantages offered by Cu-Al2O3 hybrid nanoparticles, providing valuable insights into their thermophysical properties. Additionally, Roșca, N.C. [3] reported that the use of hybrid nanofluids results in enhanced thermal conductivity, thereby improving heat transfer efficiency in heat exchangers. Yashkun, U. [4] and colleagues discussed the application of hybrid nanofluids in the context of stretching and shrinking sheets, considering the influence of radiation on heat transfer processes.

Lund and colleagues [5] delved into the examination of viscous dissipation within Cu–Al2 O3 /H2 O nanofluids comprising hybrid nano-materials over a shrinking surface. Meanwhile, Roy and coauthors [6] explored the characteristics of second-grade hybrid nanofluids. Khashi'Ie et al. [7-10] undertook a thorough investigation of permeable power-law deformable plates subjected to orthogonal shear in hybrid nanofluids. Khan and team [11] conducted a study on MHD hybrid nanofluid flow with heat sources/sinks over a stretching or shrinking sheet, utilizing slip conditions to analyze the flow for both slip and non-slip scenarios using the HAM method. Additionally, several researchers [12-18] have focused their efforts on assessing the physical properties of diverse nanofluids.

2. Mathematical Formulation

A detailed analysis is performed to investigate the heat transfer characteristics of hybrid nanofluid flow while taking into account suction and infusion factors. The fundamental model depicting this scenario is illustrated in Figure 1, where the velocity components are denoted as u in the x-direction and v in the y-direction.

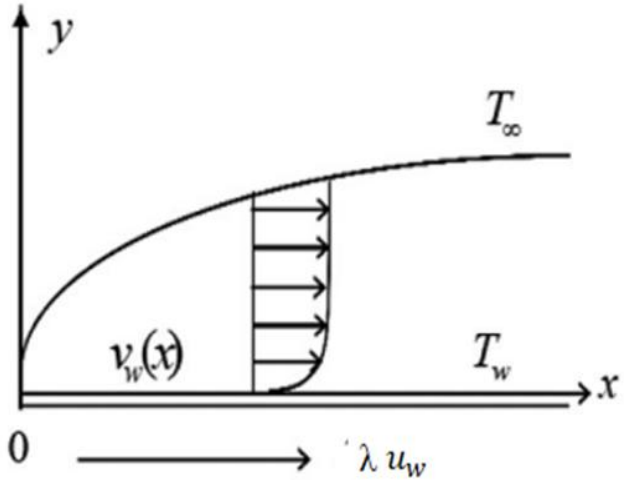

Figure 1. Physical model of problem:stretching surface ($\lambda > 0$)

Given the boundary-layer assumptions mentioned, the continuity equations as well as the equations for momentum and energy are formulated as follows [42].

$$\frac{\partial u}{\partial x}+\frac{\partial v}{\partial y}=0 \qquad (1)$$

$$u\frac{\partial u}{\partial x}+v\frac{\partial v}{\partial y}-U_e\frac{\partial U_e}{\partial x}=\frac{\mu_{hnf}}{\rho_{hnf}}\frac{\partial^2 u}{\partial y^2}-\frac{\sigma_{hnf}}{\rho_{hnf}}B_0^2(u-U_e)+\frac{\nu_{hnf}}{K\,\rho_{hnf}}(u-U_e) \qquad (2)$$

$$u\frac{\partial T}{\partial x}+v\frac{\partial T}{\partial y}=\frac{k_{hnf}}{(\rho C_p)_{hnf}}\frac{\partial^2 T}{\partial y^2}+\frac{q}{(\rho C_p)_{hnf}}(T-T_\infty)-\frac{i}{(\rho C_p)_{hnf}}\frac{\partial q_r}{\partial y} \qquad (3)$$

ISSN PRINT 2319 1775 Online 2320 7876
 Volume 11, Sp.Iss 6 , 2022

Using boundary conditions in [**43**]

$$u=cx+A_1\frac{\partial u}{\partial y},\ v=v_w,\ T=T_w(x)+B_1\frac{\partial T}{\partial y}\ at\ y=0, u\longrightarrow U_e, T\longrightarrow T_\infty\ as\ y\longrightarrow\infty \qquad (4)$$

A1 and B1 represent the slip factors for velocity and thermal energy, respectively. The correlations for the physical properties, as detailed by Tayebi et al. [44] and Takabi et al. [45], and the thermo-physical properties of the hybrid nanofluid, as presented by Oztop et al. [46], are shown in Tables 1 and 2, respectively. The radiative heat flux q_r is associated with the Rosseland [49] approximation technique.

$$q_r=\frac{-4\sigma^*}{3k^*}\frac{\partial T^4}{\partial y}$$

k^* and σ^*representsthe coefficient of mean absorption and Steepen-Bolzman constant, $T^4\approx 4T_\infty^3T-3T_\infty^4$

In the equations above, "hnf" represents the hybrid nanofluid, "f" pertains to the base fluid, "s1" represents the solid copper nanoparticles, and "s2" refers to the solid alumina nanoparticles. Furthermore, "ϕ_1 " and "ϕ_2 " symbolize the volume fraction parameters for alumina and copper, respectively.

Table 1. Hybrid nanofluid physical properties.

Properties	**Hybrid Nanofluid Correlation**
Density	$\rho_{hnf}=\rho_{s1}\phi_1+\rho_{s2}\phi_2+\rho_f(1-\emptyset_{hnf})$where $\emptyset_{hnf}=\phi_1+\phi_2$
Heat Capacity	$(\rho C_p)_{hnf}=(\rho C_p)_{s1}\phi_1+(\rho C_p)_{s2}\phi_2+(\rho C_p)_f(1-\emptyset_{hnf})$
Dynamic Viscosity	$\frac{\mu_{hnf}}{\mu_f}=1/(1-\emptyset_{hnf})^{2.5}$
Electrical Conductivity	$\frac{\sigma_{hnf}}{\sigma_f}=\frac{\left(\frac{\phi_1\sigma_{s1}+\phi_2\sigma_{s2}}{\emptyset_{hnf}}\right)+2\sigma_f+2(\phi_1\sigma_{s1}+\phi_2\sigma_{s2})-2\emptyset_{hnf}\sigma_f}{\left(\frac{\phi_1\sigma_{s1}+\phi_2\sigma_{s2}}{\emptyset_{hnf}}\right)+2\sigma_f-2(\phi_1\sigma_{s1}+\phi_2\sigma_{s2})-2\emptyset_{hnf}\sigma_f}$
Thermal Conductivity	$\frac{k_{hnf}}{k_f}=\left[\frac{2k_f+\{(\phi_1k_{s1}+\phi_2k_{s2})/\emptyset_{hnf}\}+2(\phi_1k_{s1}+\phi_2k_{s2})-2\emptyset_{hnf}k_f}{2k_f-(\phi_1k_{s1}+\phi_2k_{s2})+(\phi_1k_{s1}+\phi_2k_{s2})/\emptyset_{hnf}+\emptyset_{hnf}k_f}\right]$

Table 2. Thermophysical properties.

Physical Properties	**Base fluid H_2O**	**Cu**	**Al_2O_3**
$\rho(kg/m^3)$	1053	8933	3970
$C_p(J/kgK)$	3594	385	765
K(W/mK)	0.492	400	40

As to reduce the above-mentioned governing Equations (2) – (4), the following similarity variables are used (Waini et al. [47]).

$$\text{u= ax}f'(\eta)\ \text{v=}-\sqrt{2\nu_f}f(\eta)\theta(\eta)=\frac{T-T_\infty}{T_w-T_\infty},\ \eta=y\sqrt{\frac{a}{\nu_f}}. \qquad (5)$$

ISSN PRINT 2319 1775 Online 2320 7876
Research paper **© 2012 IJFANS. All Rights Reserved**, Volume 11, Sp.Iss 6 , 2022

These accordingly fulfil Equation (1) and transform Equations (2) and (3) into the succeeding equations.

$$\left(\frac{\mu_{hnf}/\mu_f}{\rho_{hnf}/\rho_f}\right) f''' + ff'' - (f')^2 - \frac{\mu_{hnf}/\mu_f}{\rho_{hnf}/\rho_f}(M+P)f' = 0 \quad (6)$$

$$\frac{1}{Pr}\left(\frac{k_{hnf}}{k_f} + \frac{4}{3}R\right)\theta'' + \frac{(\rho C_p)_{hnf}}{(\rho C_p)_f}(f\theta' - f'\theta) + \beta\theta = 0 \quad (7)$$

Due to the transmuted boundary conditions,

$$f(0) = S,\ f'(0) = \lambda + Af''(0),\ \theta(0) = 1 + B\theta'(0), f'(\infty) = 1,\ \theta(\infty) = 0, \quad (8)$$

such that $Pr = (\mu C_p)_f/kf$represents the Prandtl number,$R=\frac{4\sigma^* T_\infty^3}{K^*(\rho C_p)_{hnf}}$is the radiation parameter,

$\beta = q_0/c(\rho C_p)_f$illustrates the heat generation parameter, A = $A_1 U_\infty \sqrt{\frac{c}{\nu_f}}$indicates the velocity_slip_parameter$P = \upsilon_f/ck^*$ is the porosity-parameter

B = $B_1 \frac{U_\infty}{\nu_f}$indicates the thermal slip parameter, and $S = -\nu_0/\sqrt{\nu_f c}$refers to the mass transfer parameter of the wall, in which S > 0 (ν_0< 0) is related with mass suction and S < 0 (ν_0> 0) is related with mass injection.

The main physical quantities of attention (local skin_friction_coefficient $C_f$and the Nusselt_number Nu_x) are mathematically calculated as in [47].

$$C_f = \frac{\mu_{hnf}}{\rho_f}\frac{1}{u_w^2}\left(\frac{\partial u}{\partial y}\right)_{y=0}, Nu_x = \frac{k_{hnf}}{k_f}\frac{-1}{(T_w - T_\infty)}\left(\frac{\partial T}{\partial y}\right)_{y=0}, \quad (9)$$

by representing the transformation, we have the following equations,

$$Re_x^{1/2} C_f = \left(\frac{\mu_{hnf}}{\mu_f}\right) f''(0), Re_x^{1/2} Nu_x = -\left(\frac{\mu_{hnf}}{\mu_f}\right)\theta'(0), \quad (10)$$

where $Re_x = u_w/\nu_f$ represents the local Reynolds_number.

3. Results and Discussions

The numerical solutions for equations (6), (7), and (8) under the specified conditions were computed using the bvp4c method with a shooting technique within MATLAB software. Both stretching_sheet (λ > 0) and shrinking_sheet (λ < 0) scenarios were considered. A Prandtl number (Pr) of 6.2 was applied for water as the base fluid, assuming a room temperature of 25°C. The study investigated the effects of various parameters such as the Heat Generation parameter (β), Velocity Slip parameter (A), Thermal Radiation parameter (R), Thermal Slip parameter (B), Porosity parameter (P), and Suction parameter (S) on the velocity and temperature profiles of the fluid flow.

The results were validated by comparing them with the HAM method, and a reasonable correlation was observed between the current numerical results and the HAM results. Figures 2 and 3 depict the velocity variations influenced by the Magnetic parameter (M) and Porosity parameter (P). An important observation is that the velocity gradually

ISSN PRINT 2319 1775 Online 2320 7876
Research paper Volume 11, Sp.Iss 6 , 2022

increases for $0 \leq \eta \leq 2.5$ and decreases for $2.5 \leq \eta \leq 5$ as M increases. Figures 4 and 5 illustrate the velocity contours under the influence of the Suction parameter (S) and Velocity Slip parameter (A). The velocity profiles of the fluid are enhanced with increasing values of A and S. Furthermore, the increase in the volume fraction parameters of alumina and copper (ϕ_1 and ϕ_2) results in a reduction in the fluid flow velocity, as demonstrated in Figures 6 and 7..

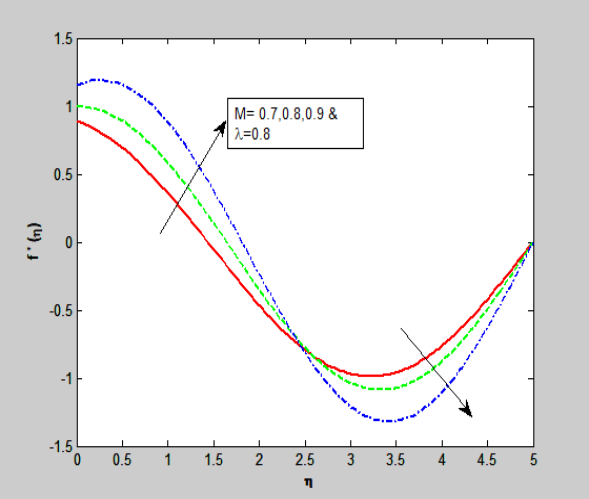

FIGURE 2. Velocity profiles for M

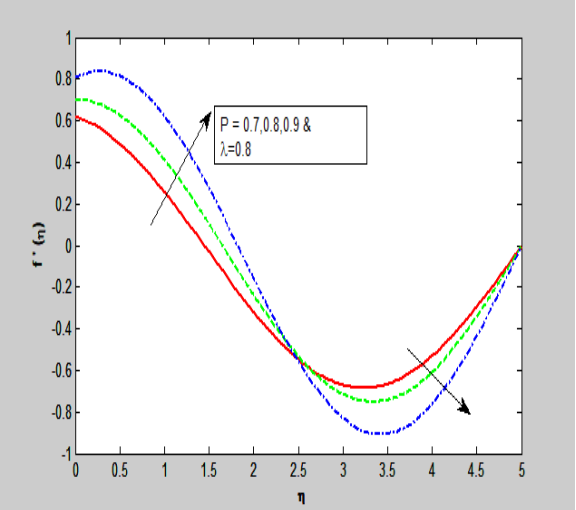

FIGURE 3. Velocity profiles for P

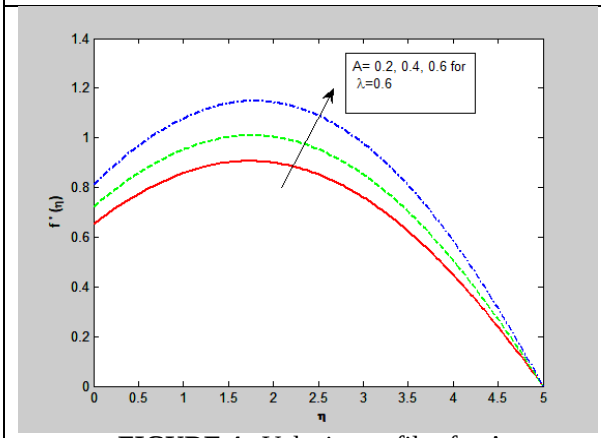

FIGURE 4. Velocity profiles for A

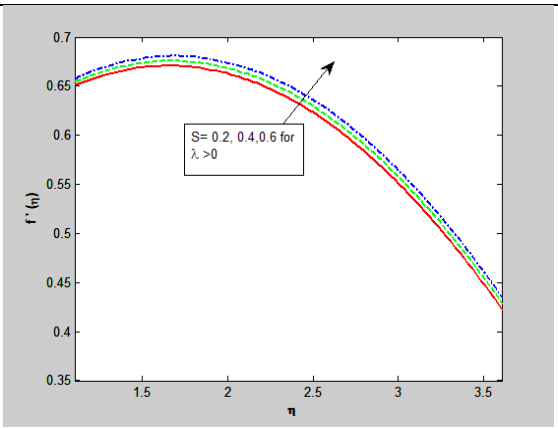

FIGURE 5. Velocity profiles for S

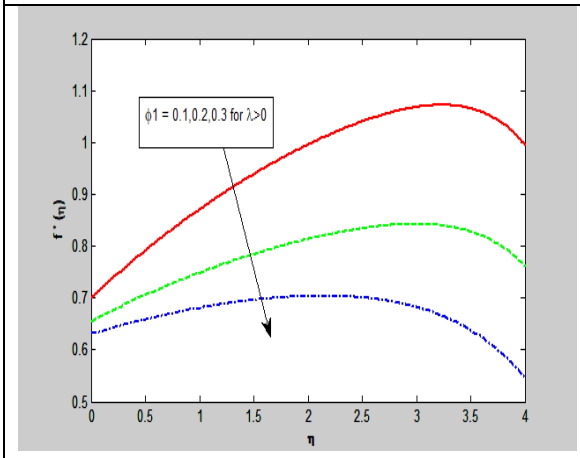

FIGURE 6. Velocity profiles for ϕ_1

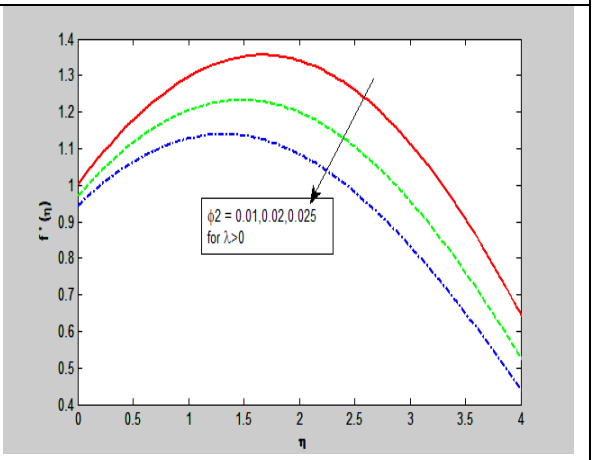

FIGURE 7. Velocity profiles for ϕ_2

ISSN PRINT 2319 1775 Online 2320 7876
 Volume 11, Sp.Iss 6 , 2022

Temperature profiles for a stretching sheet ($\lambda > 0$) are provided in Figures 8 to 15. The fluid temperature, $\theta(\eta)$, increases as the values of M, P, B, and Pr decrease, as depicted in Figures 8, 9, 10, 11, and 15. Figures 12 to 14 display the influence of the Heat Generation parameter (β), Radiation parameter (R), and volume fraction parameters for alumina and copper (ϕ_1 and ϕ_2) on the temperature contours of the fluid. It is noticeable that the temperature, $\theta(\eta)$, rises with increasing values of β, ϕ_1 and ϕ_2 .

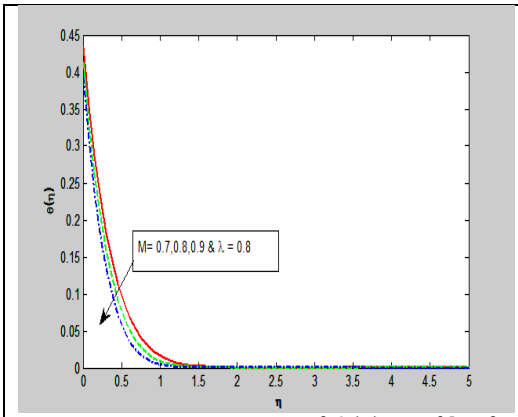

FIGURE 8. Variations of $\theta(\eta)$ profiles for M

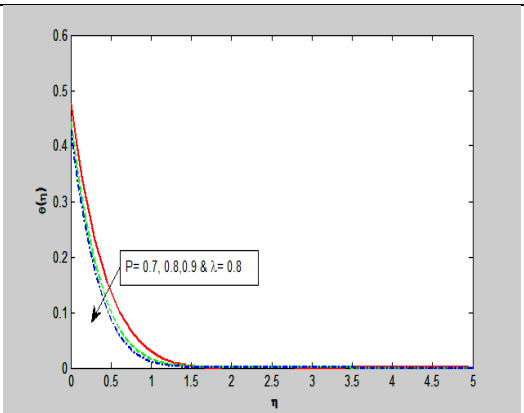

FIGURE 9. Variations of $\theta(\eta)$ profiles for P

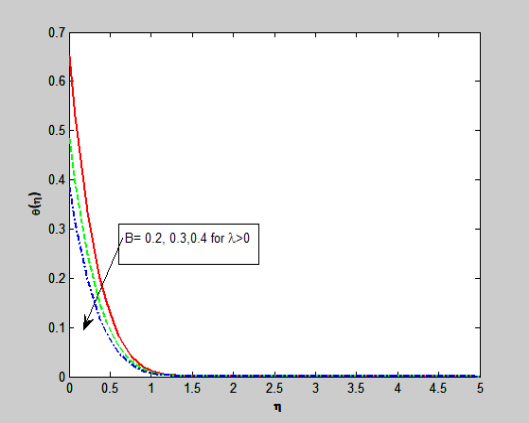

FIGURE 10. Variations of $\theta(\eta)$ profiles for B

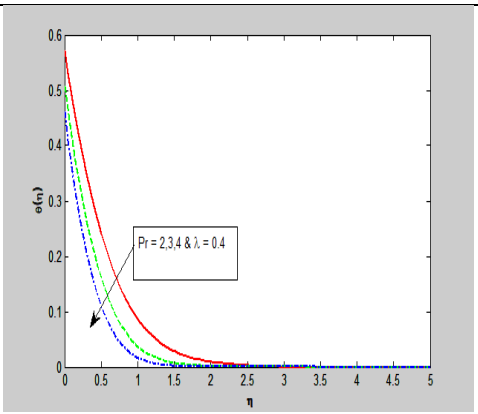

FIGURE 11. Variations of $\theta(\eta)$ profiles for Pr

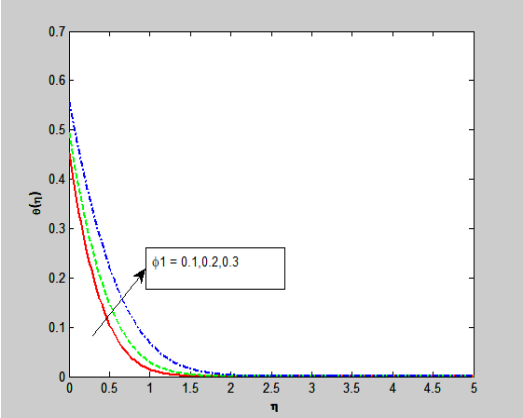

FIGURE 12. Variations of $\theta(\eta)$ profiles for ϕ_1

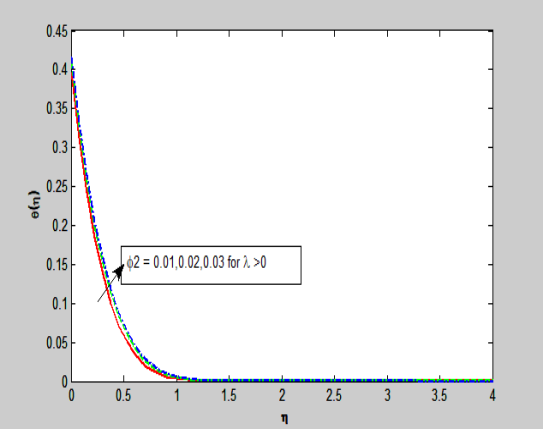

FIGURE 13. Variations of $\theta(\eta)$ profiles for ϕ_2

ISSN PRINT 2319 1775 Online 2320 7876
Research paper Volume 11, Sp.Iss 6 , 2022

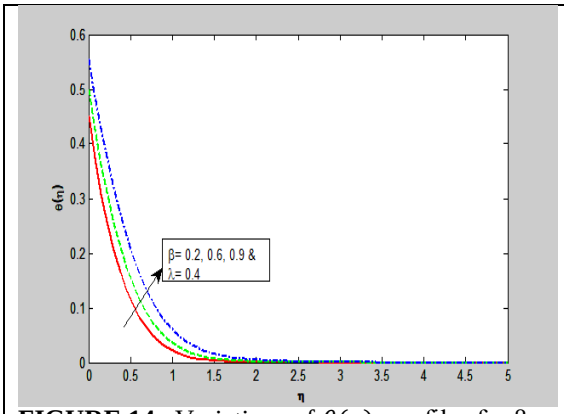

FIGURE 14. Variations of $\theta(\eta)$ profiles for β

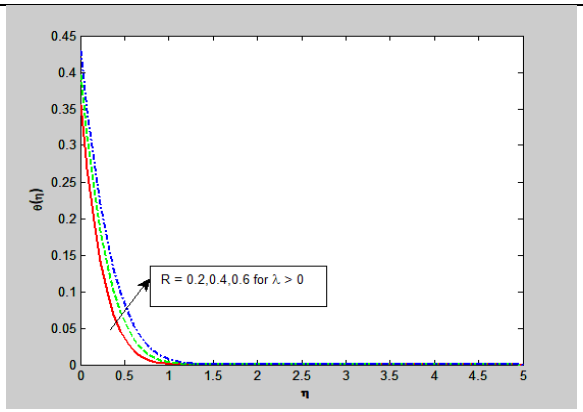

FIGURE 15. Variations of $\theta(\eta)$ profiles for R

TABLE 3: Comparison of Nu_x for different values of Pr with R = P = 0

S	Abdul Samad Khan et al [4]	Present result	Absolute error
0	0.31225	0.31229	0.00004
1	0.32272	0.32275	0.00003
2	0.32728	0.32735	0.00007
3	0.33224	0.33235	0.00011

The numerical solutions were compared with those presented by Abdul Samad Khan et al [4] and are summarized in Table 3, which provides values for the Nusselt number and skin friction coefficient in Table 4.

Table.4: Influence of different pertinent parameter(s) on C_f&Nu_x

M	P	Pr	A	B	S	β	R	$Re_x^{1/2}C_f$	$Nu_x Re_x^{-1/2}$
0.7								-0.222807	1.13272
0.8								0.001072	1.174021
0.9								0.303117	1.215134
	0.7							-0.152139	1.048849
	0.8							0.004443	1.08586
	0.9							0.216967	1.138853
		2						0.645101	0.854772
		3						0.6451	0.98444
		4						0.645101	1.077926
			0.2					0.273404	1.109091
			0.4					0.307392	1.130566
			0.6					0.353435	1.155354
				0.2				0.328486	1.738206
				0.4				0.328486	1.289814
				0.6				0.328486	1.025319
					0.1			0.324123	0.788075
					0.2			0.325369	0.873194
					0.3			0.3266	0.946846
						0.2		0.166373	1.094647
						0.6		0.166373	0.98388
						0.9		0.166373	0.808461

ISSN PRINT 2319 1775 Online 2320 7876
 Volume 11, Sp.Iss 6 , 2022

							0.2	0.480296	1.288464
							0.4	0.480296	1.20698
							0.6	0.480296	1.141728

4. Conclusion

In this paper, the Numerical solutions to find the impacts of the thermal behaviour of Cu-Al2O3/H2O when the physical parameters like magnetic field(M), Heat generation parameter (β), velocity slip parameter(A), Thermal radiation parameter (R), Thermal Slip parameter(B), Porosity parameter(P) and suction parameter(S) are embedded. The investigation of thermal parameters of hybrid nanofluid flow are presented as follows

- The velocity increases when the values of A and S are escalated.
- The velocity decrease when the values of ϕ_1 and ϕ_2 are increase.
- The temperature diminishes when the values of M and P escalate.
- The temperature increase and concentration increase when the values of ϕ_1 and ϕ_2 escalate.
- The Nusselt number increase and when the values of Pr escalate.
- The temperature diminishes and when the values of S, B and Pr escalate

5. REFERENCES

1. Maxwell, J.C. A *Treatise on Electricity and Magnetism*; Clarendon Press: Oxford, UK, (1873).
2. Hamilton, R.L.; Crosser, O.K. Thermal Conductivity of Heterogeneous Two-Component Systems. *Ind. Eng. Chem. Fundam.*(1962) 1, 187–191.
3. Ro¸sca, N.C.; Ro¸sca, A.V.; Jafari Moghaddam, A.; Pop, I. "Cross flow and heat transfer past a permeable stretching/shrinking sheet in a hybrid nanofluid". *Int. J. Numer. Methods Heat Fluid Flow* (2021), 31, 1295–1319.
4. Yashkun, U.; Zaimi, K.; Abu Bakar, N.A.; Ishak, A.; Pop, I. "MHD hybrid nanofluid flow over a permeable stretching/shrinking sheet with thermal radiation effect". *Int. J. Numer. Methods Heat Fluid Flow* (2021), 31, 1014–1031.
5. Lund, L.A.; Omar, Z. et al. "Stability analysis and multiple solution of Cu–Al2O3/H2O nanofluid contains hybrid nanomaterials over a shrinking surface in the presence of viscous dissipation." *J. Mater. Res. Technol.* (2020), 9, 421–432.
6. Roy, N.C.; Pop, I. "Flow and heat transfer of a second-grade hybrid nanofluid over a permeable stretching/shrinking sheet". *Eur. Phys. J. Plus* (2020), 135, 1–19.
7. N.S.; Arifin, N.M.; Pop, I.; Nazar, R. "Melting heat transfer in hybrid nanofluid flow along a moving surface". *J. Therm. Anal. Calorim.* (2020), 1–12.
8. Khashi'ie, N.S.; Md Arifin, N.; Pop, I. "Mixed Convective Stagnation Point Flow towards a Vertical Riga Plate in Hybrid Cu-Al2O3/Water Nanofluid". *Mathematics* (2020), 8, 912.
9. Khan, A.S.; Xu, H.-Y.; Khan, W. "Magnetohydrodynamic Hybrid Nanofluid Flow Past an Exponentially Stretching Sheet with Slip Conditions". *Mathematics* (2021), 9, 3291. https://doi.org/10.3390/ math9243291.
10. Radha Madhavi, M., Nalleboyina, V., & Nagesh, P. "Influence of magnetic field, heat radiation and external surface temperature on nanofluids with different base fluids in mixed convective flows over a vertical circular cylinder". *International Journal of Innovative Technology and Exploring Engineering*, (2019),8(5), 497-504.
11. M.Radha Madhavi. et al. "Impacts of Thermophoresis, Joule heating and Soret& Dufour effects on mixed convective Jeffery fluid flow over an elongated sheet" *International Journal of Advanced Science and Technology*, (2020),Vol. 29, No. 5, pp. 3060 – 3069.
12. Vijaya, N., Madhavi, M. R., & Krishna, Y. H. "Boundary layer of a mixed convective nanofluid flowing over a vertical circular cylinder under the influence of magnetic field, heat radiation and outside surface temperature". *International Journal of Mechanical and Production Engineering Research and Development*, (2018,)8, pp. 411-420.
13. G. Dharmaiah, W. Sridhar, K. S. Balamurugan & K. Chandra Kala, "Hall and ion slip impact on magneto-titanium alloy nanoliquid with diffusion thermo and radiation absorption", *International Journal of Ambient Energy*, (2020) DOI: 10.1080/01430750.2020.1831597
14. Hymavathi, T. and Sridhar, W.,"Numerical study of flow and heat transfer of Casson fluid over an exponentially porous stretching surface in presence of thermal radiation" *International Journal of Mechanical and Production Engineering Research and Development*,8(4),2018,1145-1154, 10.24247/ijmperdaug2018118.

ISSN PRINT 2319 1775 Online 2320 7876
 Volume 11, Sp.Iss 6 , 2022

15. M.Radha Madhavi. et al. "Mixed convective flows on Al2O3 – Engine oil nano fluid under the influence of thermal radiation &magnetic field over a vertical circular cylinder" *Test Engineering &management*, March - April (2020), ISSN: 0193-4120, Volume 83,Page No. 10891 – 10899.